Selective Permeation of Hydrocarbon Gases in Poly(tetrafluoroethylene) and Poly(fluoroethylene–Propylene) Copolymer

N. YI-YAN, R. M. FELDER,* and W. J. KOROS, *Department of Chemical Engineering, North Carolina State University, Raleigh, North Carolina 27650*

Synopsis

The permeabilities and diffusivities of methane, ethane, propane, *n*-butane, and isobutane in commercially available poly(tetrafluoroethylene) (TFE) and poly(fluoroethylene–propylene) (FEP) Teflon have been measured in a Pasternak-type permeation cell. Experiments were carried out at upstream hydrocarbon partial pressures up to 50 torr (1000–60,000 ppm gas phase concentration) and temperatures from 40 to 195°C with films of 0.0508 and 0.127 mm thickness using nitrogen as carrier gas on the upstream and downstream sides of the membrane. The transient and steady-state permeation data are described well by a combination of Henry's law and Fick's law with a concentration-independent diffusion coefficient. Linear Arrhenius plots of both permeabilities and diffusivities were obtained. Linear correlations were found both between the activation energy for diffusion and the square of the gas molecule diameter, and between the logarithm of solubility at 90°C and the penetrant boiling point. Separation factors for binary mixtures of hydrocarbons were measured for TFE at 140°C and found to be similar to those predicted by individual permeabilities in most cases. Measurements with mixed gases were not made for FEP Teflon, but selectivities of FEP are expected to be similarly well described by the ratios of the pure gas permeabilities at the low partial pressures studied. The effect of annealing FEP Teflon for 24 hr at 200°C was found to produce an average of 20–30% reduction in solubility as well as a 9% increase in the activation energy for diffusion compared to as-received films. These effects are believed to be due to increased crystallinity in the sample upon annealing.

INTRODUCTION

The diffusive transport of hydrocarbon gases in polymers has important applications in the generation of instrument calibration gases and in continuous stack-gas monitoring. The use of a permeable polymeric interface between a stack gas and a continuous analyzer has been shown to serve several functions, the most important of which are to provide a sample gas with a pollutant concentration within the optimal range of the analyzer, to screen out solid particulates and potentially corrosive acid mist, and to screen out water to an extent sufficient to preclude condensation in the sample gas line and analyzer.[1–3]

An ongoing project at North Carolina State University involves the design and characterization of polymer interfaces for the selective monitoring of hydrocarbons in process plant stacks. As a part of this project, the transport properties of methane, ethane, propane, *n*-butane, and isobutane in poly(tetrafluoroethylene) (TFE) and poly(fluoroethylene–propylene) (FEP) Teflon have been measured in a continuous permeation cell. The primary objectives of the study were to obtain the properties needed to design interfaces for monitoring emissions

* To whom correspondence should be addressed.

Journal of Applied Polymer Science, Vol. 25, 1755–1774 (1980)

0021-8995/80/0025-1755$02.00

of these species and to determine whether the species permeate independently of one another. (Independent permeation implies that single-species calibration parameters may be used to analyze data obtained for hydrocarbon mixtures.) Another objective was to study the long-term thermal stability of Teflon interfaces, specifically by determining the effect of thermal annealing on transport properties.

MEASUREMENT OF TRANSPORT PROPERTIES IN A CONTINUOUS-FLOW PERMEATION CHAMBER

In a continuous permeation experiment, a penetrant is introduced at a partial pressure p_1 on one side of a flat membrane and permeates through the polymer into a gas stream flowing past the other side of the membrane.[1-6] The concentration of the penetrant in the exiting gas is monitored continuously until a steady state is attained. In such experiments the concentration of the dissolved gas at the downstream membrane surface is negligible compared to that on the side where the penetrant was introduced. Moreover, if Henry's law describes sorption equilibrium between the gas in the upstream chamber and the polymer at the upstream surface and if Fick's law, with a constant diffusion coefficient, describes transport at a fixed temperature, the steady-state permeability defined by

$$P = F_s h/p_1 \tag{1}$$

where F_s is the steady-state flux and h is the membrane thickness, is equal to the product of the Bunsen solubility constant S and the diffusion coefficient, D, i.e.,

$$P = SD \tag{2}$$

From eq. (1), the permeability can be obtained as the slope of an isothermal plot of F_s vs. p_1/h.

While the permeability is obtained from the steady-state flux, the diffusivity is obtained from the membrane transient response. Let $F(h,t)$ be the measured flux at the downstream surface of the polymer at a time t, and define M_0 (the zero moment of the response) as

$$M_0 = \int_0^\infty \left(1 - \frac{F(h,t)}{F_s}\right) dt \tag{3}$$

Felder, Spence, and Ferrell[5] have shown that for a flat membrane and constant diffusivity, M_0 is identical to the time lag $h^2/6D$, so that

$$D = h^2/6M_0 \tag{4}$$

Dynamic measurements of the type described above yield the response of the entire system (connecting lines, chamber, polymer, and gas analyzer) to a step concentration change upstream of the membrane. To evaluate the diffusivity from eqs. (3) and (4), the response of the polymer alone is required. If $R(t)$ is the measured response of the entire system to a step concentration change, R_s is the steady-state value of this response, and

$$M_0' = \int_0^\infty \left(1 - \frac{R(t)}{R_s}\right) dt \tag{5}$$

the correct value of M_0 to use in eqs. (3) and (4) has been shown by Felder, Ma, and Ferrell[6] to be

$$M_0 = M_0' - (\tau_1 + \tau_2 + \tau_3 + \tau_a) \tag{6}$$

where τ_1 and τ_2 are the mean residence times of the gas in the line leading to the chamber and in the chamber itself, respectively; τ_3 is the mean residence time of the carrier gas in the line leading from the chamber to the analyzer; and τ_a is the delay owing to the analyzer. (In the present study, the need to determine τ_a was eliminated by recording the time of sample injection rather than the time of the measured signal.)

Permeabilities and diffusivities of gas in polymers are well known to follow Arrhenius relations over moderate temperature ranges[7]

$$P = P_0 \exp(-E_p/RT) \tag{7}$$

$$D = D_0 \exp(-E_D/RT) \tag{8}$$

From eqs. (2), (7), and (8) it follows that

$$S = P/D = S_0 \exp(-\Delta H_s/RT) \tag{9}$$

where P_0, D_p, and S_0 are preexponential factors, E_p is the apparent activation energy for permeation, E_D is the activation energy for diffusion, ΔH_s is the apparent heat of solution, T is the absolute temperature, and R is the universal gas constant.

In the case of mixtures of penetrants, the degree of separation through the membrane permeation process is commonly expressed in terms of a separation factor α_{ij}, which is defined by the following concentration ratio[8]:

$$\alpha_{ij} = \frac{Y_i/Y_j}{X_i/X_j} \tag{10}$$

where Y_i and Y_j are the downstream mole fractions of the ith and jth components. If the concentration of penetrant at the downstream membrane boundary is maintained negligibly small relative to the upstream concentration, and if the assumptions of Fickian diffusion and Henry's law sorption remain valid for all components and the components permeate independently of one another, the separation factor α_{ij} is equivalent to the ratio of the individual permeabilities

$$\alpha_{ij,p} = P_i/P_j \tag{11}$$

In the present study these conditions are satisfied: the upstream penetrant concentration varied from 1000 to 60,000 ppm while the downstream penetrant concentration never exceeded 5 ppm. A comparison of α_{ij} and $\alpha_{ij,p}$ thus gives an indication of the occurrence of interactions among the components of a penetrant mixture.

EXPERIMENTAL

Apparatus

The continuous-flow permeation chamber is constructed of 304 stainless steel and consists of two cylindrical compartments (i.d. = 50.8 mm, o.d. = 76.2 mm) with the membrane sealed between by means of an O ring. A C clamp is used to hold the two halves of the cell together. Each compartment has tangential ports for the inlet and outflow of the span gas (upstream compartment) or carrier gas (downstream compartment). Two additional ports are drilled in the upstream compartment for the monitoring of the chamber temperature and pressure by a copper-constantan thermocouple and a mercury manometer, respectively. Prior to the outset of a run, the chamber is placed in a thermostatically controlled oven (Fisher Isotemp forced-draft oven, model 350) and connected to the remainder of the experimental apparatus.

A schematic diagram of the flow apparatus is shown in Figure 1. All lines in the system are constructed of 6.35-mm-o.d. copper tubing and brass fittings with the exception of the portions between the oven inlet and outlet valves which are constructed of 6.35-mm-o.d. 304 stainless steel tubing and 316 stainless steel fittings. All valves used are made of 316 stainless steel.

Four gases are involved in the operation of the unit. The first is the span gas (hydrocarbon in nitrogen) flowing past the upstream side of the film. The second is the conditioning gas (ultrahigh-purity-grade nitrogen) which is used either to dilute the span gas to a desired concentration in the film or to flush the upstream chamber to remove sorbed gases in the film prior to the start of an experiment. The third is the carrier gas, which is the same as the conditioning gas (nitrogen), flowing past the downstream side of the film. The fourth is the analyzer calibration gas consisting of ultrahigh-purity-grade nitrogen passing over a calibrated propane permeation tube contained in a constant temperature bath. Each of the four gas flow systems is provided with a rotameter and a mercury manometer for the measurement of flow rates and pressures.

The carrier gas emerging from the permeation chamber and the calibration gas are sent to the gas analyzer through a three-way valve; while one of these

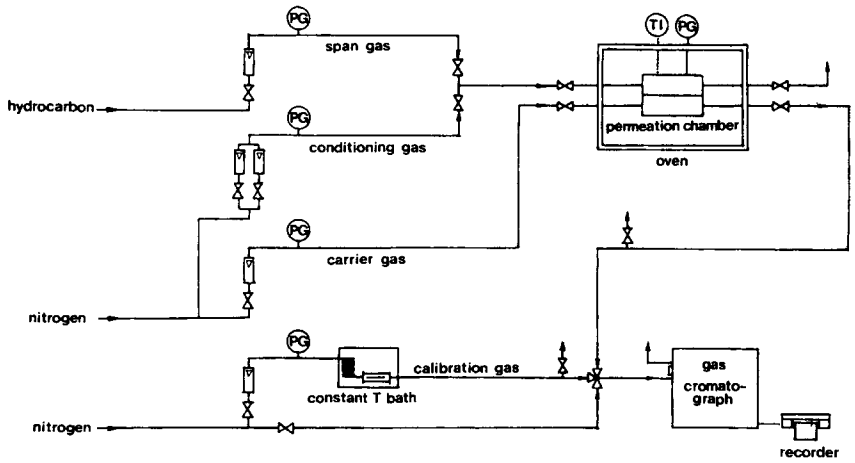

Fig. 1. Diagram of experimental apparatus.

streams is being analyzed, the other is vented. Additionally, the pure nitrogen used for calibration purposes is connected to the three-way valve for occasional checks for contaminants in this stream (none were detected during the present study).

The gas analyzer is a Shimadzu gas chromatograph, model 6AM, with dual-flame ionization detectors. The reference and working columns were packed with squalane. Ultrahigh-purity-grade nitrogen was supplied as the reference column gas and the sample carrier gas. The gas chromatograph was calibrated before and after each experimental run using the calibration gas described above. The responses of the detector were measured with a Shimadzu bench-type automatic balancing recorder.

Materials

The hydrocarbons used as span gases were primary standards of 5 or 6 mole % of methane, ethane, propane, *n*-butane, or isobutane in nitrogen supplied by Air Products, Inc. Cylinders of different concentrations of a given species were used to check data reproducibility. The ultrahigh-purity-grade nitrogen used in the system was also supplied by Air Products, Inc.

The membranes used were TFE Teflon of 0.127 mm thickness and FEP Teflon (type A) of 0.127 and 0.0508 mm thicknesses, both provided by the Livingston Coating Corporation of Charlotte, North Carolina. Each film was annealed for 24 hr at 200°C; no deterioration or significant change in thickness was observed. FEP films were also used in the "as-received" state to evaluate differences in transport properties owing to annealing.

Transport Property Measurements

The membrane is sealed between the two compartments of the permeation chamber, which in turn is connected to the feed and effluent lines inside the oven. The apparatus is pressure tested for leaks. Next, the oven thermostat is set and the chamber temperature is monitored until it reaches steady state. Meanwhile, the upstream and downstream chambers are flushed with nitrogen to eliminate any residual hydrocarbon in the membrane. Then, the flow rates of the span gas and dilution gas are adjusted to provide the desired penetrant concentration in the upstream chamber, and the flow rate of the carrier gas is adjusted to provide a sample gas with a hydrocarbon concentration within the range of the flame ionization detector. The total pressure on both sides of the film is maintained at approximately 1 atm.

The sampling of the carrier gas begins when the span gas flow commences, and the run continues until steady-state permeation is achieved. Continued sampling during the steady-state permeation process then permits accurate determination of the steady-state permeation flux at the hydrocarbon partial pressure being tested. The hydrocarbon concentration in the sample gas, which is proportional to the penetrant flux, is then substituted into eq. (5) to obtain M_0'. The time lags τ_1, τ_2, and τ_3 attributed to the connecting lines and chamber are calculated from the known volumes of these components and the corresponding

volumetric flow rates, and the lag owing to the polymer alone is determined from eq. (6). Finally, the diffusivity of hydrocarbon in the polymer is calculated from eq. (4).

For permeability measurements, steady-state sample gas concentrations are measured for different upstream penetrant partial pressures. These values are multiplied by the carrier gas flow rate and divided by the exposed membrane area to obtain F_s. Then, the permeability of hydrocarbon in the polymer is determined by fitting a least-squares line to a plot of F_s vs. p_1/h, according to eq. (1).

For separation factor measurements, a premixed binary mixture of hydrocarbons of known composition is passed through the upstream chamber. The steady-state concentrations in the sample gas are measured and the separation factor is calculated using eq. (10).

RESULTS AND DISCUSSION

Permeabilities of Pure Hydrocarbons

Permeabilities of methane, ethane, propane, *n*-butane, and isobutane have been measured in 0.127-mm TFE films at temperatures between 70 and 185°C and in 0.0508-mm FEP films at temperatures between 40 and 130°C, with upstream penetrant partial pressures up to 50 torr. The films used were all annealed at 200°C for 24 hr. Additionally, permeabilities of propane were measured in 0.0508-mm FEP films in the "as-received" state to evaluate differences in membrane transport properties due to annealing.

Figure 2 shows isothermal plots of F_s vs. p_1/h for propane in TFE; the slope of these plots equals the permeability at the corresponding temperature [eq. (1)]. Space does not permit presentation of similar plots for the other penetrants and membrane studied, but the data shown in Figure 2 are typical in all respects.[9] The linearity of these plots supports the assumption that in the range of upstream partial pressures used (up to 50 torr), the Henry's law–Fickian diffusion model is valid for the films and penetrant species tested.

Figures 3 and 4 show plots of the logarithm of the permeabilities versus reciprocal absolute temperatures. These plots yielded straight lines for the range of temperatures involved, indicating the applicability of the Arrhenius law [eq. (7)]. The apparent activation energies for permeation and preexponential factors derived by linear regression from the slopes and intercepts of these plots are listed in order of increasing penetrant carbon number in Table I for TFE and in Table II for FEP. The permeation data in Table II are compared with data reported by Pasternak, Burns, and Heller[10] for methane, ethane, and propane in FEP in the range 25–90°C, and by Britt[11] for ethane, propane, and *n*-butane in FEP in the range 40–183°C. The agreement is excellent among the activation energies; the permeabilities are reasonably close, the differences being easily accounted for in terms of variations between membrane samples.

From the data in Tables I and II it is evident that in both types of Teflon tested, the apparent activation energies for permeation increase with the size of the penetrant molecule. The same trends are apparent in the preexponential factors. The relative changes in E_p and P_0 lead to a decrease in the permeabilities themselves with increasing size of the penetrant molecule. This effect is illus-

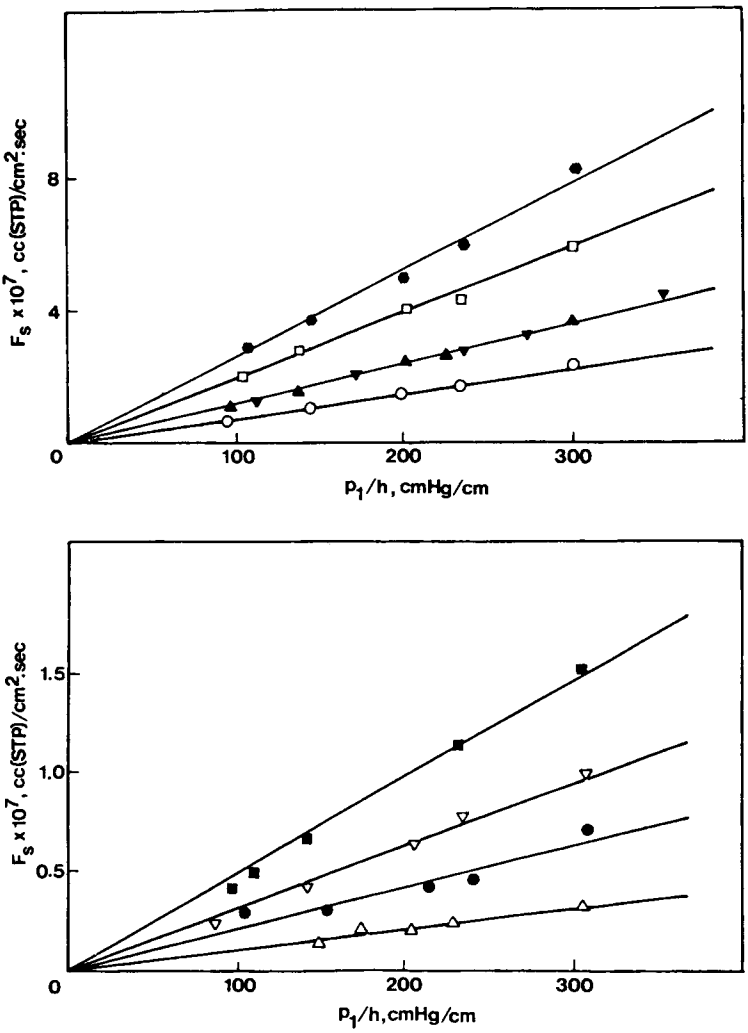

Fig. 2. Steady-state flux F_S of propane in TFE as a function of the upstream penetrant partial pressure over membrane thickness p_1/h. Temperature (°C): (●) 192.7, (□) 179.8, (▲) 158.3 (C_3 cyl. concentration, 5.06%), (▼) 158.3 (C_3 cyl. concentration, 5.99%), (○) 143.1, (■) 129.7, (▽) 115.7, (●) 100.9, (△) 84.6.

trated in Figure 5, which shows plots of permeabilities at 90°C versus the number of carbon atoms in the hydrocarbon chain. In the case of linear hydrocarbons, the permeabilities tend to level off after four carbon atoms, whereas the branched isobutane has a much lower permeability than its linear isomer. Figure 5 also shows that the permeabilities in FEP are about 60% greater than those in TFE films. Although both types of membrane show selectivity for the permeation of the hydrocarbons involved, the greater differences between the permeabilities of different species in FEP indicates a greater ability of this film to separate closely related penetrants.

A comparison of the permeation data for propane through annealed and unannealed FEP films in Table II shows that annealing has the effect of decreasing both the permeability and the apparent activation energy for permeation. This

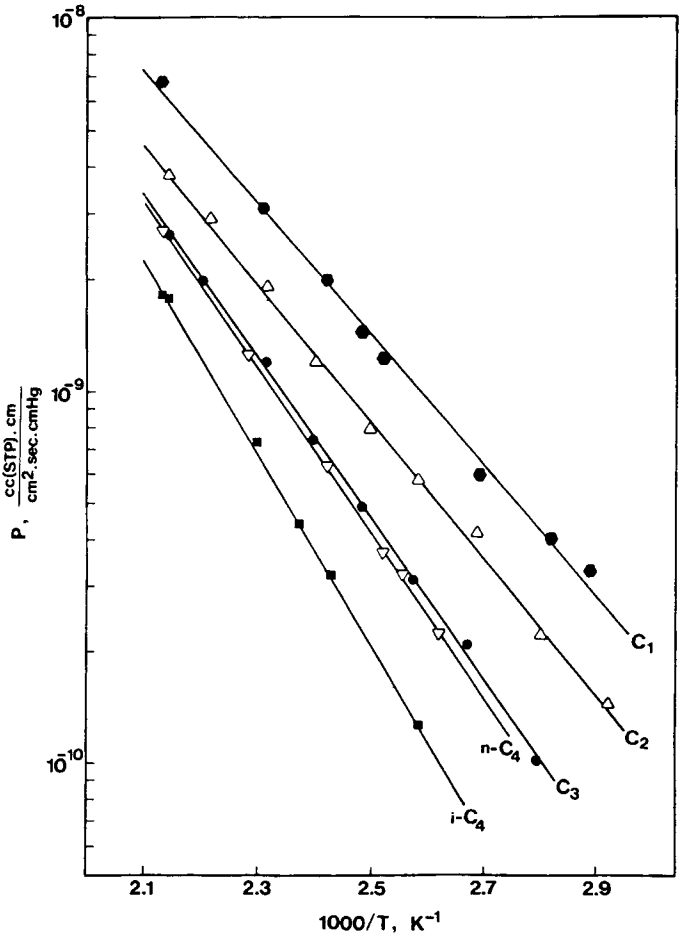

Fig. 3. Logarithm of the permeability P of hydrocarbon gases in TFE as a function of the reciprocal temperature $1/T$. (●) Methane, (△) ethane, (●) propane, (▽) n-butane, (■) isobutane.

TABLE I
Permeation Data for Hydrocarbon Gases in TFE[a]

Hydrocarbon	E_P	P_0	$P_{90°C} \times 10^{10}$
Methane	8.06	3.64×10^{-5}	5.13
Ethane	8.42	3.34×10^{-5}	2.86
Propane	9.94	1.23×10^{-4}	1.28
n-Butane	10.21	1.63×10^{-4}	1.17
Isobutane	11.84	6.18×10^{-4}	0.46

[a] E_P in kcal/g mole; P_0 and $P_{90°C}$ in [cm^3(STP) cm]/(cm^2 sec cm Hg).

effect might be ascribed to a variation in the crystalline content of the membrane after annealing. Owing to the composite nature of P [eq. (3)], this postulate is better discussed in terms of effects on the individual diffusivity and solubility parameters, so it will be reconsidered in the sections that follow. The annealed membranes showed excellent transport stability with no change in permeability or diffusivity noted after prolonged exposure to elevated temperatures (<200°C) for well over two weeks.

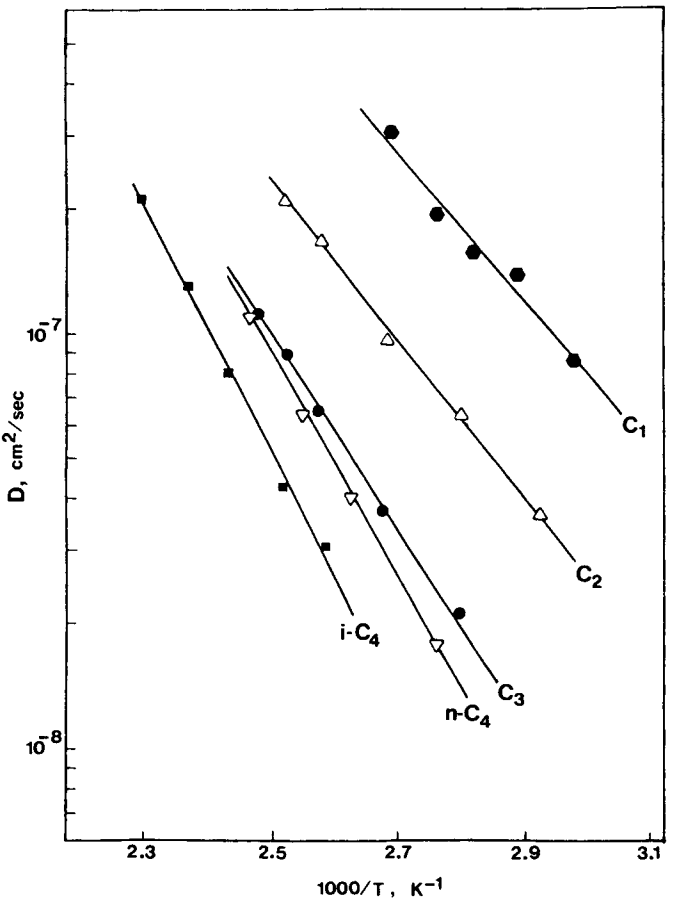

Fig. 4. Logarithm of the permeability P of hydrocarbon gases in FEP as a function of the reciprocal temperature $1/T$. (O) Propane, unannealed film; other symbols as in Fig. 3.

Diffusivities

Diffusivities of methane, ethane, propane, n-butane, and isobutane have been measured in TFE and FEP films at temperatures between 30 and 130°C with upstream penetrant partial pressures up to 50 torr. In the case of TFE, all measurements were made in 0.127-mm annealed films. For the diffusion of methane, ethane, and propane at the highest temperatures, annealed 0.127-mm films had to be used, since steady-state permeation was reached too quickly in the thinner membrane to allow the precise determination of the diffusion coefficients. Diffusivities of propane through unannealed 0.0508-mm FEP films were also measured for comparison. Each recorded diffusivity was the mean of at least two experiments at the same temperature and different partial pressures of the penetrant on the upstream side. The diffusivities so obtained agreed within the precision of the measurements, with no trends observed in relation to the upstream penetrant concentration. This result proves the concentration independence of D for the penetrant partial pressures of 50 torr and less used in these measurements.

Figures 6 and 7 show plots of the logarithm of the measured diffusivities versus reciprocal absolute temperature. Similar to the permeabilities, the diffusivities

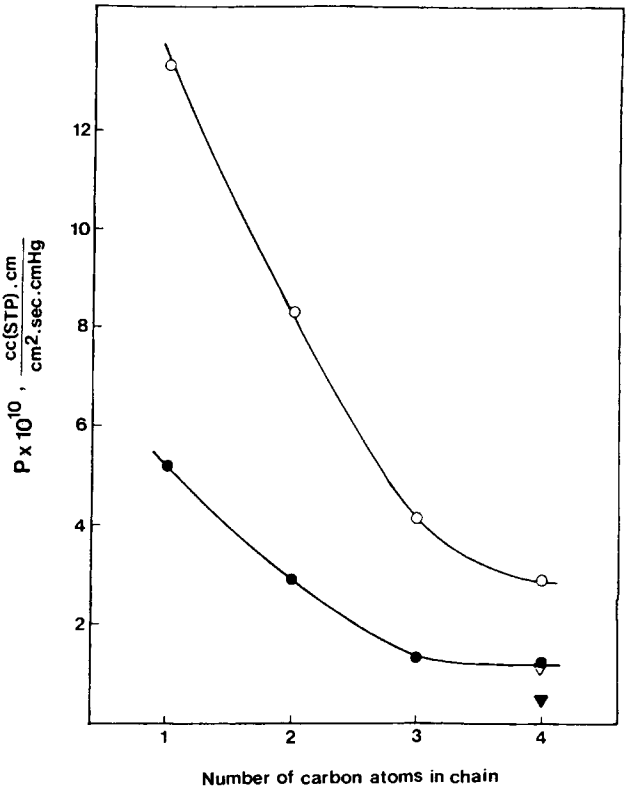

Fig. 5. Permeability $P_{90°C}$ at 90°C as a function of the number of carbon atoms in the hydrocarbon chain. (●) *n*-Paraffins in TFE, (▼) isobutane in TFE, (○) *n*-paraffins in FEP, (▽) isobutane in FEP.

depend on temperature according to the Arrhenius type of relationship [eq. (8)] for the range of temperatures involved. The measured diffusivities do not appear to vary with the FEP film thickness, as shown by the values for ethane at temperatures around 70°C in Figure 7.

The ideal nature of the transport behavior observed in these experiments, in which Fick's law and Henry's law are valid and diffusion is an activated process, is characteristic of systems in which there is little interaction between the gas and the polymer. Since the partial pressures of penetrant used at the upstream side of the membrane were relatively small, the small quantity of gas dissolved in the polymer did not affect the structure of the polymer. The activation energies for diffusion and the preexponential factors derived from the least-squares lines contained in Figures 6 and 7 are listed in order of increasing penetrant carbon number in Table III for TFE and in Table IV for FEP. Diffusion data reported by Pasternak et al.[10] and Britt[11] have been included in Table IV for comparison. The agreement is again good among the activation energies. The diffusivities determined in the present study are close to those measured by Britt, while the values given by Pasternak et al. are somewhat larger. Such small variations, however, are not unexpected, since gas transport behavior is sensitive to the detailed nature of the polymer structure, composition and morphology, factors that vary from membrane to membrane.

TABLE II
Permeation Data for Hydrocarbon Gases in FEP[a]

Hydrocarbon	Present study			Britt (ref. 11)		Pasternak et al. (ref. 10)	
	E_P	P_0	$P_{90°C} \times 10^{10}$	E_P	$P_{90°C} \times 10^{10}$	E_P	$P_{90°C} \times 10^{10}$
Methane	8.37	1.45×10^{-4}	13.30			8.31	10.96
Ethane	8.80	1.62×10^{-4}	8.30	9.03	6.91	8.74	6.32
Propane	10.48	8.40×10^{-4}	4.14	9.87	3.34	10.29	3.23
n-Butane	12.94	1.78×10^{-2}	2.90	11.56	3.02		
Isobutane	16.10	0.56	1.14				
Propane in unannealed film	11.71	8.12×10^{-3}	7.54				

[a] E_P in kcal/g mole; P_0 and $P_{90°C}$ in [cm^3(STP) cm]/(cm^2 sec cm Hg).

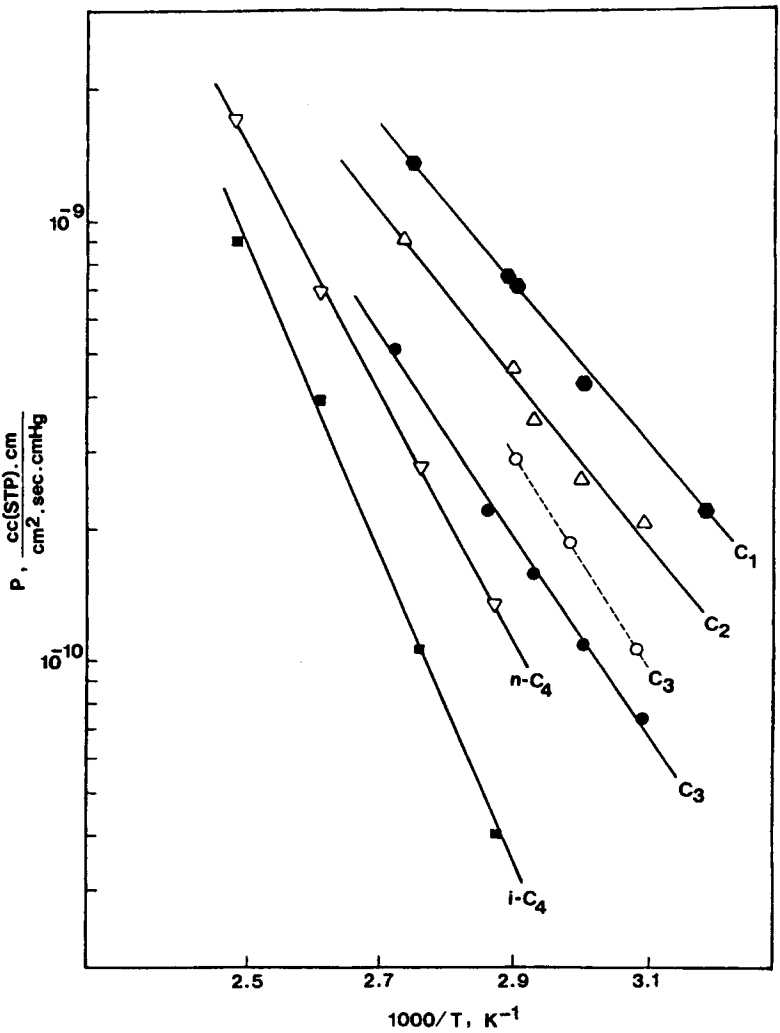

Fig. 6. Logarithm of the diffusivity D of hydrocarbon gases in TFE as a function of the reciprocal temperature $1/T$. Symbols as in Fig. 3.

TABLE III
Diffusion Data for Hydrocarbon Gases in TFE

Hydrocarbon	E_D (kcal/g mole)	D_0 (cm²/sec)	$D_{90°C} \times 10^8$
Methane	8.28	2.13×10^{-2}	22.13
Ethane	8.64	1.21×10^{-2}	7.63
Propane	10.70	6.92×10^{-2}	2.51
n-Butane	12.29	0.47	1.87
Isobutane	13.87	1.92	0.86

Data from Tables III and IV show E_D and D_0 to increase with the size of the diffusing molecule in accordance with Eyring's theory of activated diffusion.[4] The activation energies for diffusion correlates with d, the diameter of the gas molecules obtained from gas viscosity data in Reid, Prausnitz, and Sherwood[12]

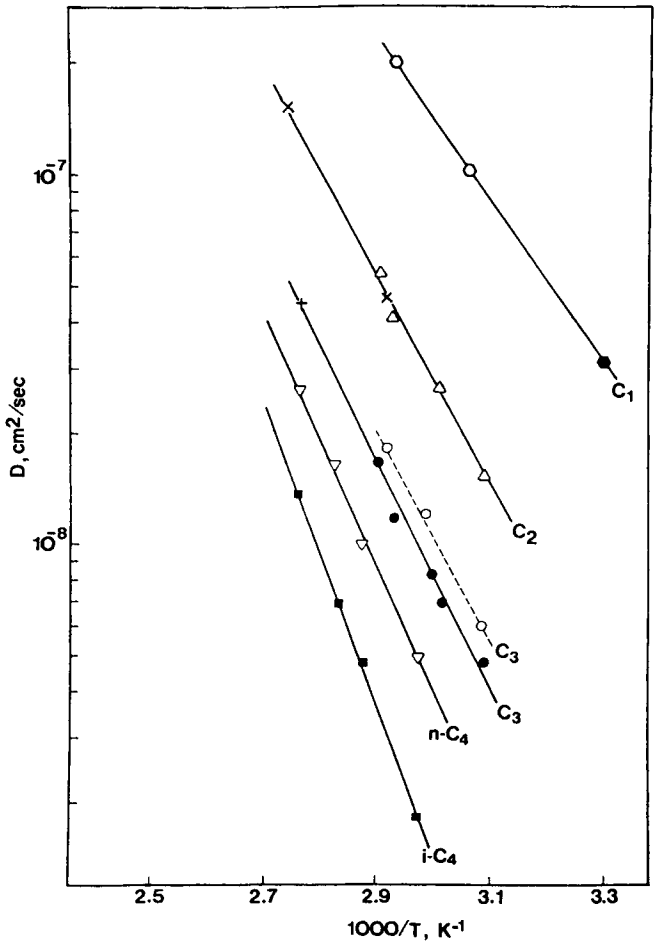

Fig. 7. Logarithm of the diffusivity D of hydrocarbon gases in FEP as a function of the reciprocal temperature $1/T$. (●) Methane, 0.0508-mm film; (○) methane, 0.127-mm film; (△) ethane, 0.0508-mm film; (X) ethane, 0.127-mm film; (●) propane, 0.0508-mm film; (+) propane, 0.0508-mm film (unannealed); (▽) n-butane, 0.0508-mm film; (■) isobutane, 0.0508-mm film.

and listed in Table V. Fairly linear relations were obtained when plotting E_D vs. d^2, as illustrated in Figure 8, with the following equations applying:

$$E_D(\text{TFE}) = 0.483d^2 \tag{12}$$

$$E_D(\text{FEP}) = 0.641d^2 \tag{13}$$

Theoretical interpretations of the second-order dependence of E_D on d have been discussed by Meares.[13] No attempt has been made to correlate the preexponential factors with d. The uncertainty in the values of D_0 are quite large because their determination involved a linear extrapolation for different intervals of $1/T$ (an uncertainty of 0.05 kcal in E_D may result in an uncertainty of 7% in the preexponential factor). The values of D_0 should therefore be used only for the prediction of diffusivities by substitution in eq. (8).

The slower diffusion process for larger molecules, which is due to their larger activation energies, is reflected in decreasing diffusivities with increasing molecular size. This fact is illustrated in Figure 9, where diffusivities at 90°C have

TABLE IV
Diffusion Data for Hydrocarbon Gases in FEP[a]

Hydrocarbon	Present study			Britt (ref. 11)		Pasternak et al. (ref. 10)	
	E_D	D_0	$D_{90°C} \times 10^8$	E_D	$D_{90°C} \times 10^8$	E_D	$D_{90°C} \times 10^8$
Methane	9.87	0.43	49.09			10.89	83.14
Ethane	12.86	7.71	14.03	12.60	14.53	12.35	20.34
Propane	14.20	17.20	4.89	14.87	4.66	14.37	6.16
n-Butane	15.52	60.90	2.78	15.38	2.46		
Isobutane	18.58	2230	1.46				
Propane in unannealed film	13.0	3.42	5.13				

[a] E_D in kcal/g mole; D_0 and $D_{90°C}$ in cm^2/sec.

TABLE V
Molecule Diameters and Boiling Points of Hydrocarbon Gases

Hydrocarbon	d (Å)	T_b (K)
Methane	3.758	112
Ethane	4.443	184
Propane	5.518	231
n-Butane	4.687	272
Isobutane	5.278	261

been plotted against the number of carbon atoms in the hydrocarbon chain. As does the permeability, D tends to level off after four carbon atoms. Also, branching has a greater effect on lowering the value of D than does increasing chain length. The latter result was also found by Prager and Long[14] for the diffusion of hydrocarbons in polyisobutylene. From Figure 9, it is also evident that the diffusivities of the hydrocarbons tested are greater in FEP than in TFE by about 45%.

A comparison of the diffusion data for propane through annealed and unannealed FEP films in Table IV shows that annealing leads to an increase in the value of E_D, and a decrease in the diffusivity. This result is reasonable, considering that a semicrystalline polymer (such as FEP) can be regarded as interspersed crystalline and amorphous regions, where the crystallites act as impermeable fillers that increase the tortuosity of the diffusion path and may also act as crosslinking agents that restrain the mobility of neighboring chain segments.[15] Annealing might have produced an increase in the crystalline content of the membrane, so that a greater activation energy and more time is required for the gas molecules to diffuse through the annealed film.

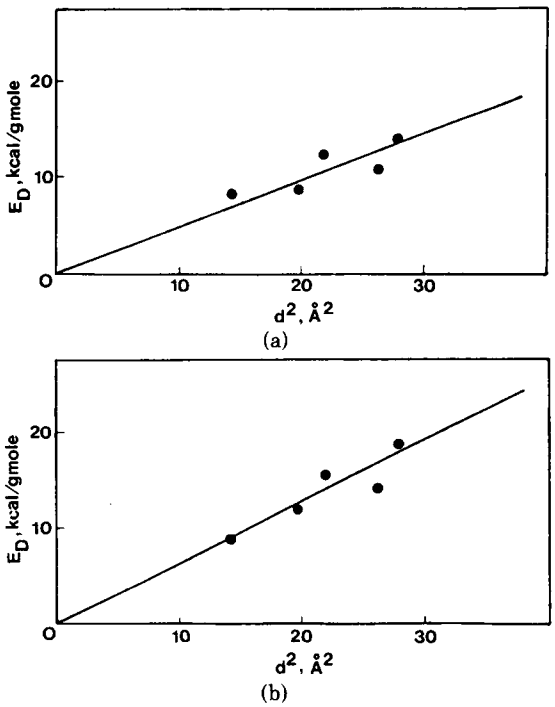

Fig. 8. Activation energy for diffusion E_D as a function of the gas molecule diam. d. (a) $E_{D,\mathrm{TFE}} = 0.483d^2$; (b) $E_{D,\mathrm{FEP}} = 0.641d^2$.

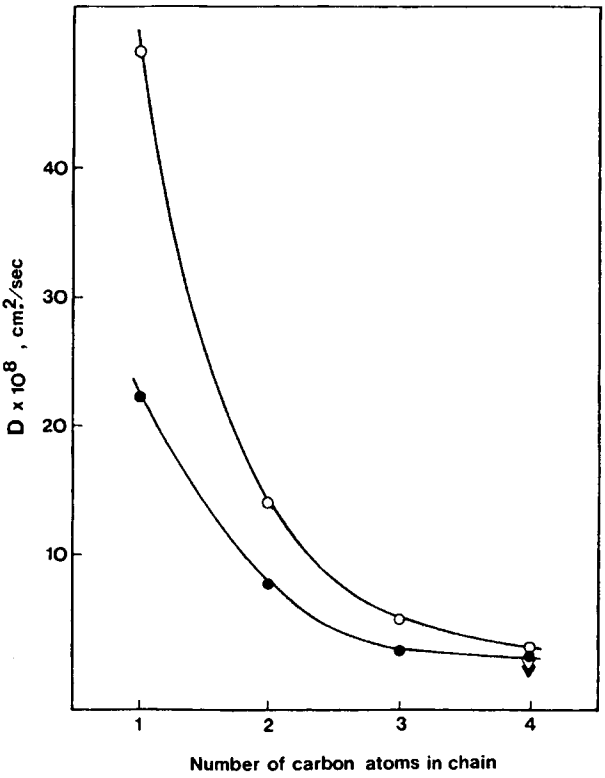

Fig. 9. Diffusivity $D_{90°C}$ at 90°C as a function of the number carbon atoms in the hydrocarbon chain. In TFE, (●) n-paraffins and (▼) isobutane; in FEP, (○) n-paraffins and (▽) isobutane.

Solubilities

Tables VI and VII contain the estimation formulas for the solubilities of hydrocarbons in FEP and TFE, respectively. These formulas have been derived using eq. (9) and the data contained in Tables I through IV. Apparent heats of sorption deduced from these formulas involve some uncertainty because ΔH_s must be calculated as the difference between the activation energies, E_p and E_D, both of which are of similar magnitudes. The estimated solubilities at 90°C also included in Tables VI and VII show these values to increase with the number of carbon atoms in the straight chain hydrocarbons, while the solubility of isobutane falls between the solubilities of propane and n-butane. Also, the solubilities of hydrocarbons in FEP are greater than those in TFE, presumably as

TABLE VI
Solubility Data for Hydrocarbon Gases in TFE[a]

Hydrocarbon	S	$S_{90°C} \times 10^3$
Methane	$1.71 \times 10^{-3} \exp(110.7/T)$	2.32
Ethane	$2.76 \times 10^{-3} \exp(110.7/T)$	3.74
Propane	$1.78 \times 10^{-3} \exp(382.5/T)$	5.16
n-Butane	$3.50 \times 10^{-4} \exp(1047/T)$	6.25
Isobutane	$3.22 \times 10^{-4} \exp(1022/T)$	5.37

[a] S and $S_{90°C}$ in cm^3(STP)/(cm^3 cm Hg), T in K.

TABLE VII
Solubility Data for Hydrocarbon Gases in FEP[a]

Hydrocarbon	S	$S_{90°C} \times 10^3$
Methane	$3.39 \times 10^{-4} \exp(755/T)$	2.86
Ethane	$2.10 \times 10^{-5} \exp(2048/T)$	5.83
Propane	$4.88 \times 10^{-5} \exp(1872/T)$	8.50
n-Butane	$2.92 \times 10^{-4} \exp(1298/T)$	10.40
Isobutane	$2.51 \times 10^{-4} \exp(1248/T)$	7.81
Propane in unannealed film	$2.37 \times 10^{-3} \exp(654/T)$	14.35

[a] S and $S_{90°C}$ in $cm^3(STP)/(cm^3\ cm\ Hg)$, T in K.

a result of a less ordered structure in FEP, which is a branched copolymer. This fact, along with the greater diffusivities through FEP, accounts for the higher permeabilities observed for this film in relation to TFE.

The solubility of gas is related to its tendency to condense, of which the boiling point T_b, critical temperature T_c, and Lennard–Jones force constant ϵ/K are each measures. The logarithm of the solubility has been found to be a linear function of T_b and T_c[16] and of ϵ/K.[17] Since all three parameters are measures of the van der Waals interaction forces of gases and differ only by approximately constant factors ($T_b \simeq 0.6T_c$ by the Guldberg–Guye rule and $T_c \simeq 0.3\epsilon/K$), the ensuing discussion has been limited to T_b. Table V lists the boiling points (from Perry's Handbook[8]) of the different hydrocarbons used, and Figure 10 shows plots of the logarithm of the solubilities at 90°C versus these boiling points. The plots yielded straight lines with the following equations applying:

$$\log S_{90°}(\text{TFE}) = -6.72 + 5.99 \times 10^{-3}T_b \tag{14}$$

$$\log S_{90°}(\text{FEP}) = -6.69 + 7.74 \times 10^{-3}T_b \tag{15}$$

On the other hand, the solubility in a semicrystalline polymer depends on the volume fraction of the amorphous region, since the gas molecules are assumed to be soluble only in such regions. Table VII shows the solubility of propane in unannealed FEP to be greater than in the annealed film. This fact suggests once more that annealing increases the crystalline content of the film. An examination of the films by x-ray diffraction might confirm this observation, although this was not done in the present study.

Separation Factors

Separation factors of binary mixtures of methane, ethane, propane, n-butane, and isobutane were measured in TFE at 140°C using eq. (12). Individual permeabilities were also measured under the same conditions and the predicted separation factors were calculated using eq. (13). The results from these runs are compiled in Table VIII. Figure 11 shows a plot of α_{ij} vs. $\alpha_{ij,p}$. It is observed that in most cases, the points fall within or very close to the diagonal $\alpha_{ij} = \alpha_{ij,p}$. Although the permeation of ethane seems to be slightly affected by the presence of more soluble components, the penetrants studied may in general be assumed to permeate independently of one another, since the separation factors can be predicted well from the individual permeabilities.

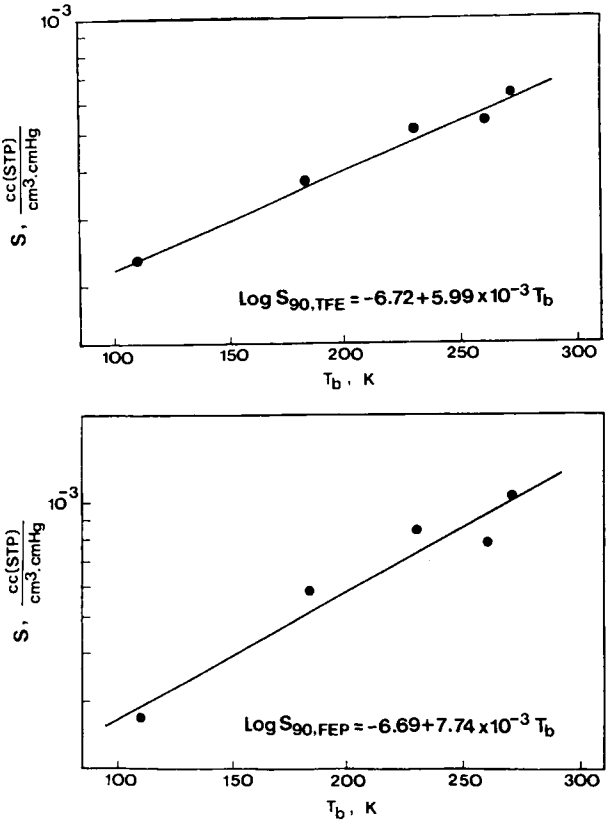

Fig. 10. Logarithm of the solubility $S_{90°C}$ as a function of the boiling point T_b.

CONCLUSIONS

The permeation of methane, ethane, propane, butane, and isobutane through TFE and FEP Teflon, at penetrant partial pressures up to 50 torr and at temperatures between 40 and 195°C, follows the Henry's law–Fickian diffusion model. The temperature dependencies of the diffusivity and permeability follow

TABLE VIII
Measured and Predicted Separation Factors in TFE at 140°C

Symbol (Fig. 11)	Mixture i-j	α_{ij}	$\alpha_{ij,P}$
●	Methane–ethane	1.85	1.76
○	Methane–propane	3.05	2.99
■	Methane–n-butane	3.33	3.33
△	Methane–isobutane	6.89	6.76
●	Ethane–propane	1.47	1.70
○	Ethane–n-butane	1.62	1.89
▼	Ethane–isobutane	3.06	3.84
▽	Propane–n-butane	1.23	1.11
■	Propane–isobutane	2.30	2.26
□	n-Butane–isobutane	2.24	2.03

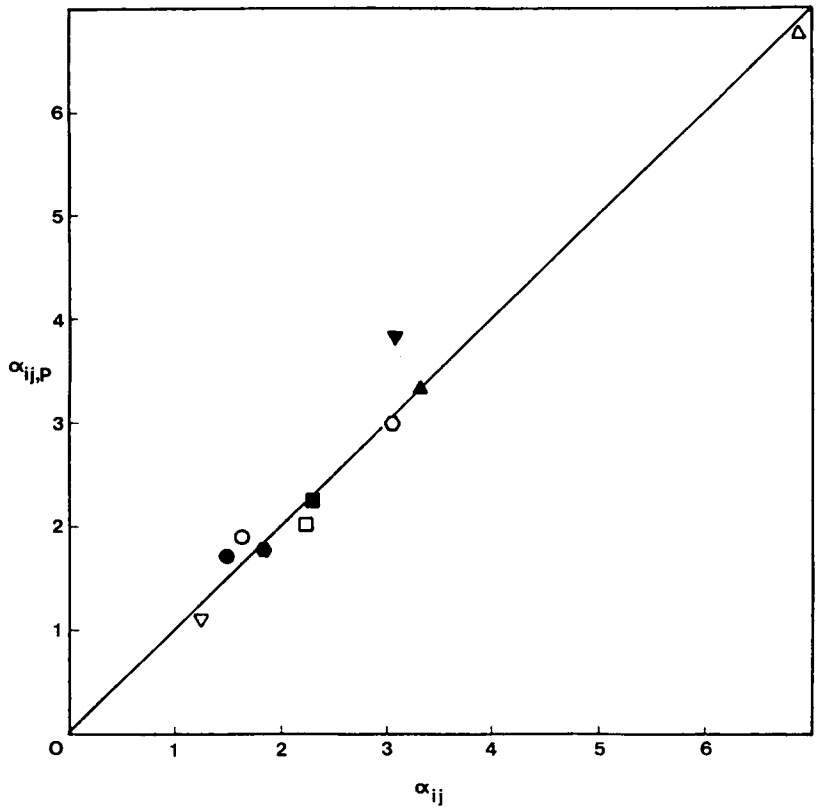

Fig. 11. Measured vs. predicted separation factors of binary mixtures of hydrocarbons in TFE at 140°C. Symbols identified in Table VIII.

Arrhenius-type relations over the temperature range studied. The activation energy for diffusion correlates linearly with the square of the penetrant gas molecule diameter, and the logarithm of the solubility of 90°C correlates linearly with the boiling points of the penetrants.

The permeabilities and diffusivities of the hydrocarbons tested have been found to be greater in FEP than in TFE Teflon. Likewise, FEP is more perm-selective than TFE for small hydrocarbons relative to large hydrocarbons.

The hydrocarbons studied can be assumed to permeate independently of one another in TFE Teflon. Although small interactions were found in a mixture of ethane and isobutane, the separation factors could still be predicted from the individual permeabilities.

Annealing on FEP film has the effect of lowering its permeability to hydrocarbons, presumably by increasing its crystalline content; such thermal treatment appears to produce a permanent "heat setting" of the transport properties of the film if use temperatures do not exceed the annealing temperature.

The authors acknowledge the support of this work under Environmental Protection Agency Grant No. R805194010.

References

1. C. E. Rodes, R. M. Felder, and J. K. Ferrell, *Environ. Sci. Technol.*, **7**, 66 (1973).
2. R. M. Felder, J. J. Spivey, and J. K. Ferrell, *Anal. Instrum.*, **12**, 35 (1974).
3. L. C. Treece, R. M. Felder, and J. K. Ferrell, *Environ. Sci. Technol.*, **10**, 457 (1976).
4. J. Crank and G. S. Park, in *Diffusion in Polymers*, J. Crank and G. S. Park, Eds., Academic, London, 1968, chap. 1.
5. R. M. Felder, R. D. Spence, and J. K. Ferrell, *J. Polym. Sci.*, **19**, 3193 (1975).
6. R. M. Felder, C-C. Ma, and J. K. Ferrell, *AIChE J.*, **22**, 724 (1976).
7. V. Stannett, in *Diffusion in Polymers*, J. Crank and G. S. Park, Eds., Academic, London, 1968, chap. 2.
8. R. A. Perry and C. H. Chilton, *Chemical Engineering Handbook*, 5th ed. McGraw-Hill, New York, 1973.
9. N. Yi-Yan, M. S. thesis, North Carolina State University. Raleigh, 1979.
10. R. A. Pasternak, G. L. Burns, and J. Heller, *Macromolecules*, **4**, 470 (1970).
11. T. E. Britt, M. S. thesis, North Carolina State University, Raleigh, 1978.
12. R. C. Reid, J. M. Prausnitz, and T. K. Sherwood, *The Properties of Gases and Liquids*, McGraw-Hill, New York, 1977.
13. P. Meares, *J. Am. Chem. Soc.*, **76**, 3415 (1954).
14. S. Prager and F. A. Long, *J. Am. Chem. Soc.*, **73**, 4071 (1951).
15. A. S. Michaels and H. J. Bixler, *J. Polym. Sci*, **50**, 413 (1961).
16. G. J. Van Amerongen, *J. Polym. Sci.*, **5**, 307 (1950).
17. A. S. Michaels and H. J. Bixler, *J. Polym. Sci.*, **50**, 391 (1961).

Received January 18, 1980
Revised February 15, 1980